ROBUST, MODEL–INDEPENDENT GENERATION OF INTRINSIC CHARACTERISTICS AND MULTI–BIAS PARAMETER EXTRACTION FOR MESFETS / HEMTS

A. Ghazinour and R.H. Jansen

RWTH Aachen University of Technology, EE Department, ITHE,
Kopernikusstrasse 16, D–52074 Aachen, Germany

Abstract

This paper presents an improved, model–independent and particularly robust RF characterization and parameter extraction approach based on multi–bias S–parameters. With a new hybrid evolutionary / conjugate gradient strategy, consistent and largely start value–independent results are obtained. Devices from various MMIC foundries are used to demonstrate the quality of this approach.

Introduction

For the time– and cost–optimized development of microwave ICs, accurate modeling of the relevant active devices like MESFETs and HEMTs is essential. Multi–bias S–parameters are usually taken as the basis for deriving suitable bias–dependent small–signal RF models and, subsequently, full dynamic (large–signal) models in compact design–oriented form. However, the set of parameters of even sufficiently good small signal models – typically obtained by fitting (optimization) processes – may be start–value dependent and physically not consistent over the range of bias situations considered [1]. A helpful step to overcome part of this problem is to generate simplified models from additional DC and pinch–off measurements, for example to extract parasitic, peripheral model parameters first, before then deriving the intrinsic device parameters [2]–[4]. But, the necessary assumptions needed to do this can also be the cause of severe consistency errors [5] and the additional measured data are often not available from manufacturers.

Higher modeling consistency and efficiency is achieved by a combination of optimization and analytical extraction which considerably reduces the number of fitting parameters in the extraction procedure [5], [6]. Here, the intrinsic device parameters are computed analytically for each bias situation as a function of the peripheral, parasitic elements which are treated as global (bias–independent) data in the associated fitting process. This reduces the start–value dependency of the results along with reducing the number of optimization variables but does not generally eliminate it [7], [8]. Our experience shows, for example, that the outlined procedure still may yield negative (unphysical) values for the intrinsic series resistances Ri and Rgd in typical MESFET / HEMT models. This implies that further improvement of robustness and consistency is needed.

Building on referenced previous work [5],[6], we describe such improvements with a view towards robust, efficient and generalized device model parameter computation for MIC / MMIC design. The chosen small–signal equivalent circuit topology is sufficiently general to cover simultaneously the wide–spread models [9]-[12] by Materka, Angelov, Curtice, McCament (SPICE) and others, thus making the approach to a large extent model–independent. A common feature of the named models, also adopted here, is the approximation of bias–independent intrinsic parameters τ, Rgd, Ri and Cds which does not compromise device model quality as our investigations have revealed for a range of devices. On the other hand, our approach yields and visualizes all other intrinsic model parameters as voltage dependent quantities which can then be represented by published nonlinear equations as in [9]–[12] or by user defined resp. process–specific proprietary equations. All global parameters (bias–independent elements) are determined by a new hybrid optimization technique, merging the advantages of an evolutionary algorithm [13] with that of a conjugate gradient optimizer [14] which has been found to be a key feature for robustness resp. start–value independence. The evolutionary portion eliminates to a high extent the local minimum problem, while the conjugate gradient optimizer boosts the efficiency of the evolutionary algorithm. The intrinsic bias–dependent elements are derived individually for each bias–specific data set by analytical equations. It will be demonstrated for devices from various MMIC foundries that this provides results efficiently, accurately, physically consistent for a large operating range and widely independent from model parameter start values.

0-7803-4471-5/98/$10.00 (c) 1998 IEEE

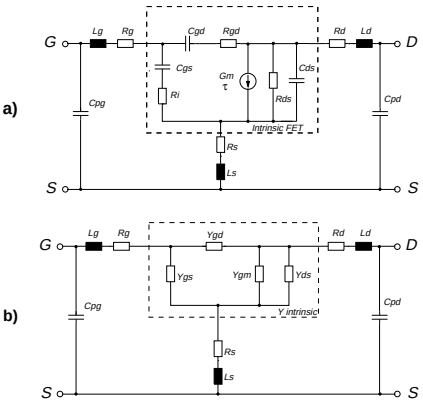

Fig. 1: **a)** Small signal equivalent circuit covering a range of common models **b)** Equivalent circuit with π–structure for the intrinsic part

Analytical derivation of bias–dependent model parameters

As outlined already, the equivalent circuit shown in Fig. 1a is well suited to accurately describe MESFETs and HEMTs at microwave and millimeterwave frequencies [10], [16]. The general structure of the intrinsic portion is a π–network as visualized in Fig. 1b with admittances, that can be computed efficiently in each step of a multi–bias fitting process as a function of the global, peripheral elements (optimization parameters). For each bias situation, the elements of Fig. 1b are computed as follows from the two–port admittance parameters Y_{ij} of the full equivalent circuit:

$$Y_{gm}=\tfrac{1}{D}\,(Y_{21}-Y_{12}) \qquad Y_{gs}=\tfrac{1}{D}\,(Y'_{11}+Y_{12}-Z_d\Delta Y')$$
$$Y_{gd}=\tfrac{-1}{D}\,(Y_{12}+Z_s\Delta Y') \qquad Y_{ds}=\tfrac{1}{D}\,(Y_{12}+Y'_{22}-Z_g\Delta Y')$$

where:

$$Y'_{11}=Y_{11}-j\omega C_{pg} \qquad Y'_{22}=Y_{22}-j\omega C_{pd}$$
$$\Delta Y'=Y'_{22}Y'_{11}-Y_{12}Y_{21} \qquad Z_k=R_k+j\omega L_k \quad (k=g,d,s)$$

$$D=1-Z_s\sum Y'_{ij}-Z_dY'_{22}-Z_gY'_{11}+\Delta Y'\sum Z$$
$$\sum Z=Z_dZ_g+Z_sZ_g+Z_dZ_s$$
$$\sum Y'_{ij}=Y'_{11}+Y_{12}+Y_{21}+Y'_{22}$$

The intrinsic bias dependent elements are derived by suitable summation over all $(l=1,2,\ldots L)$ measurement frequencies ω_l individually for each bias point:

$$C_{gs}=\tfrac{1}{L}\cdot\sum_{l=1}^{L}\frac{|Y_{gs_l}|^2}{\omega_l\cdot Im\left(Y_{gs_l}\right)} \qquad C_{gd}=\tfrac{1}{L}\cdot\sum_{l=1}^{L}\frac{|Y_{gd_l}|^2}{\omega_l\cdot Im\left(Y_{gd_l}\right)}$$

$$R_{ds}=\frac{\sum_{l=1}^{L}\frac{1}{\omega_l}}{\sum_{l=1}^{L}\frac{Re\left(Y_{ds_l}\right)}{\omega_l}} \qquad G_m=\frac{\sum_{l=1}^{L}\frac{|Y_{gm_l}\cdot(1+j\omega_l C_{gs}R_i)|}{\omega_l}}{\sum_{l=1}^{L}\frac{1}{\omega_l}}.$$

With the inverse frequency terms contained in R_{ds} and G_m an increased weighting of low frequency contributions is achieved.

Hybrid Optimization Approach

Fig. 2 shows the flow diagram of the new hybrid optimization strategy, developed and applied here. As it is characteristic for evolutionary optimization, the process starts with a population of start parameter vectors (individuals) which is improved until suitable termination criteria are satisfied. Each individual is a set of normalized parameters representing the optimization variables. A random initialization generates the components of each individual as evenly distributed random numbers in the interval [Xmin, Xmax]. In the tests described here this interval covers the large range of $0.1\cdot X_A\ldots 10\cdot X_A$ of physically relevant estimates X_A.

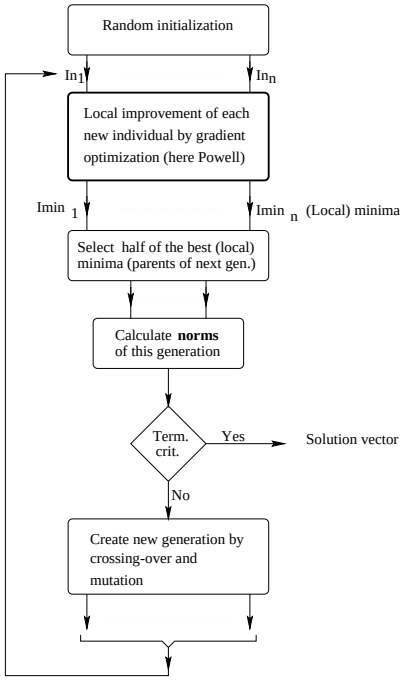

Fig. 2: Flow diagram of the hybrid optimizer

In contrast to a pure evolutionary algorithm, the hybrid optimizer of Fig. 2 uses a conjugate gradient portion [14] in addition. This is used to locally improve each individual with the available gradient information in the n–dimensional parameter space towards obtaining a local best value. Similar as in Ref. [14] it is enforced by a suitable mapping function (normalization), that the interval of $0.1\cdot X_A\ldots 10\cdot X_A$ is not left:

$$X_B=\left[1+\tanh\left(\tfrac{X-1}{3.5}+X_0\right)\right]\left(\tfrac{X_{max}-X_{min}}{2}\right)+X_{min}$$

with

$$X_0=\arctan\left(\tfrac{2-(X_{max}+X_{min})}{X_{max}-X_{min}}\right).$$

Under application of the error function Err for N bias points, with

$$Err=\tfrac{1}{4LN}\sum_{n=1}^{N}\sum_{l=1}^{L}\sum_{i,j=1}^{2}\left(\frac{\left|Smeas^n_{ij_l}-Scalc^n_{ij_l}\right|}{max\left(Smeas^n_{ij}\right)}\right)^p \quad (p\approx 1),$$

a selection is then made of the better half of the local minima (parents of the next generation) and used to generate 2 new norm–individuals each by linear and quadratic averaging of the components of the parent vectors, respectively. Once the residual er-

rors associated with the norm–individuals do not deviate substantially anymore from that of the best individual, a flat and well behaved shape of the error function in the parameter space has been obtained. More iterations do then not provide a further reduction of the error minimum, as was verified by extensive tests using random initialization. For this reason, the strategy of Fig. 2 uses as a termination criterion the deviation of the residual errors of the norm–individuals from the best fitting result obtained. If the termination criterion is not satisfied, randomly chosen individuals are used to generate new individuals.

Results

For reasons of limited space in this summary, we give only one example here for the quality, accuracy and efficiency of the developed parameter extraction approach. The device considered is a HEMT of the GEC Marconi (GMMT) Foundry, Caswell, UK, described by multi–bias S–parameters over $1 - 40GHz$. Similar high quality results have been obtained for devices of other foundries and shown in the presentation.

Table. 1 shows the parameter values and associated % standard deviations as obtained from 100 different random initializations. For a few peripheral, parasitic elements of very small numerical value a standard deviation of 15–30 % is completely acceptable. Standard deviations obtained in the order of 1% for parasitic inductances and for nearly all of the intrinsic parameters are excellent. They confirm, that the results obtained are largely independent of the randomly initiated start values.

Also, the generated parasitic values give good agreement between measured and computed S–parameters, even for a simplified Cold–Model with $Vds = 0$, though the obtained resistance values are on the low side compared to physical consideration as is the case in [5]–[7]. Naturally, the best fit between computed and measured data using a non–rigorous model compromising for design speed can not be completely in line with the true physical parasitic values [7], [15]. Moreover, the characteristics of bias dependent elements Cgs, Cgd, Gds, Gm, as shown in Figs. 3–4, demonstrate physically consistent behaviour for the whole range of bias situations considered, see [10], [17] for comparison. Finally, the residual error distribution of Fig. 5 and the S–parameters for 6 different bias situations in Fig. 6 demonstrate the excellent agreement between measured and computed data over the full frequency range of $1 - 40GHz$. The average residual error taken over all 160 bias points and the full frequency range is only 2.46%, see Fig. 5.

Conclusion

This contribution describes progress with respect to accurate, robust and consistent intrinsic device RF characterization and parameter extraction in a generalized form applicable to a wide range of MESFET / HEMT models used in industry design applications. The approach presented is based on a mixture of fitting and analytical parameter extraction, yielding and visualizing the voltage dependent intrinsic parameters in model–independent form. A key feature in this approach is a hybrid optimizer, which for a wide range of situations and devices has been tested to provide largely start value–independent results. The approach and the quality of results obtained contributes to further improving design–oriented large signal modeling and associated MMIC design quality.

Acknowledgement

Thanks are due to Dr. Mike Brookbanks of GEC Marconi, Caswell, UK, for providing the multi–bias measured S–parameter data used in this summary.

References

[1] R. L. Vaitkus, in Proc. IEEE Conf. High Speed Semiconductor Devices Circuits, Cornell Univ., pp. 301–308, 1983.

[2] R. Anholt and S. Swirhun, IEEE Trans. Microwave Theory Tech., vol. MTT–39, pp. 1243–1247, July 1991.

[3] E. Arnold, M. Golio, M. Miller, and B. Beckwith, IEEE MTT–S Int. Microwave Symp. Dig., vol. 1, pp. 359–362, May 1990.

[4] G. Dambrine, A. Cappy, F. Heliodore, and E. Playez, IEEE Trans. Microwave Theory Tech., vol. MTT–36, pp. 1151–1159, July 1988.

[5] F. Lin and G. Kompa, IEEE Trans. Microwave Theory Tech., vol. MTT–42, pp. 1114–1121, July 1994.

[6] K. Shirakawa, H. Oikawa, T. Shimura, Y. Kawasaki, Y. Ohashi, T. Saito, and Y. Daido, IEEE Trans. Microwave Theory Tech., vol. MTT–43, pp. 499–503, Mar. 1995.

[7] G. Kompa and M. Novotny, in Proc. IEEE MTT–S Workshop on Experimentally based FET Device Modelling & Related Nonlinear Circuit Design, Univ. Kassel, Germany, pp. 6.1–16, July 1997.

[8] J. A. Reynoso–Hernández, F. E. Rangel–Patiño, and J. Perdomo, IEEE Trans. Microwave Theory Tech., vol. MTT–44, pp. 2625–2633, Dec. 1996.

[9] A. Materka and T. Kacprzak, IEEE Trans. Microwave Theory Tech., vol. MTT–33, pp. 129–135, Feb. 1985.

[10] I. Angelov, H. Zirath and N. Rorsman, IEEE Trans. Microwave Theory Tech., vol. MTT–40, pp. 2258–2266, Dec. 1992.

[11] W. R. Curtice and M. Ettenberg, IEEE Trans. Microwave Theory Tech., vol. MTT–33, pp. 1383–1394, Dec. 1985.

[12] A. J. McCament, G. D. McCormack, and D. H. Smith, IEEE Trans. Microwave Theory Tech., vol. MTT–38, pp. 822–824, June 1990.

[13] T. Bäck, U. Hammel, and H. P. Schwefel, IEEE Trans. Evolu. Comp., vol. 1, pp. 3–17, Apr. 1997.

[14] R. H. Jansen et al., LINMIC+/N CAD Package, vrs. 4.1, Jansen Microwave, Aachen, Germany, May 1997.

[15] R. Anholt, in Proc. IEEE MTT–S Workshop on Experimentally based FET Device Modelling & Related Nonlinear Circuit Design, Univ. Kassel, Germany, pp. 5.1–8, July 1997.

[16] M. Berroth and R. Bosch, IEEE Trans. Microwave Theory Tech., vol. MTT–39, pp. 224–229, Feb. 1991.

[17] U. Schaper and A. Werthof, in Proc. IEEE MTT–S Workshop on Experimentally based FET Device Modelling & Related Nonlinear Circuit Design, Univ. Kassel, Germany, pp. 26.1–5, July 1997.

Parasitics	Average	% Std. Dev.
$Cpg[fF]$	5.16	15.48
$Cpd[fF]$	0.03	28.76
$Rs[\Omega]$	1.46	3.64
$Rg[\Omega]$	0.22	28.38
$Rd[\Omega]$	0.20	0.57
$Ls[pH]$	18.30	0.98
$Lg[pH]$	17.90	1.31
$Ld[pH]$	16.87	1.44
Intrinsics	Average	% Std. Dev.
$Ri[\Omega]$	4.45	3.62
$Rgd[\Omega]$	15.51	0.93
$\tau[ps]$	0.89	1.02
$Cds[fF]$	23.07	0.11
$Cgs[fF]$	83.54	1.00
$Cgd[fF]$	19.60	0.13
$Gm[mS]$	23.64	0.21
$Rds[k\Omega]$	5.65	2.12

Tab. 1: Average values and standard deviations obtained from 100 random initialisations chosen in the range of $0.1 \cdot X_A \ldots 10 \cdot X_A$.

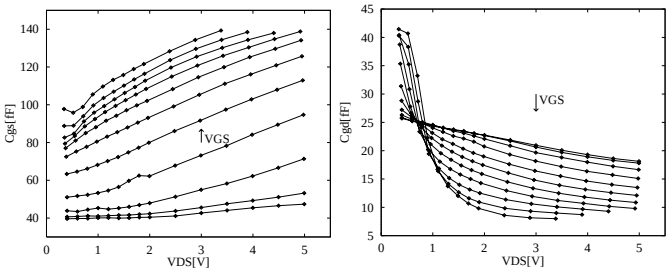

Fig. 3: Cgs and Cgd versus Vds for Vgs =-1.2V. . . 0.3V step 0.15V.

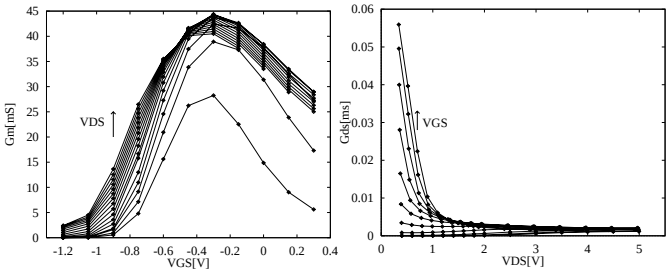

Fig. 4: Gm versus Vgs for Vds =0.3V. . . 4.8V step 0.3V and $Gds = 1/Rds$ versus Vds for Vgs =-1.2V. . . 0.3V step 0.15V.

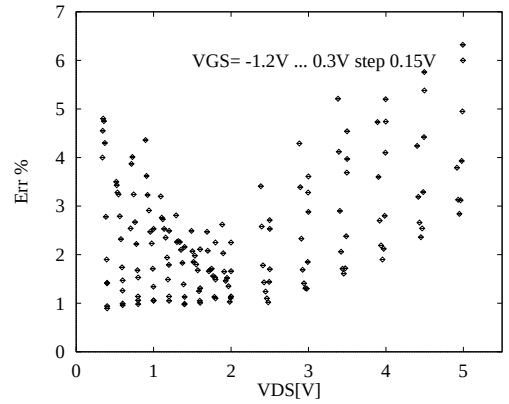

Fig. 5: S–parameter % residual error as a function of bias.

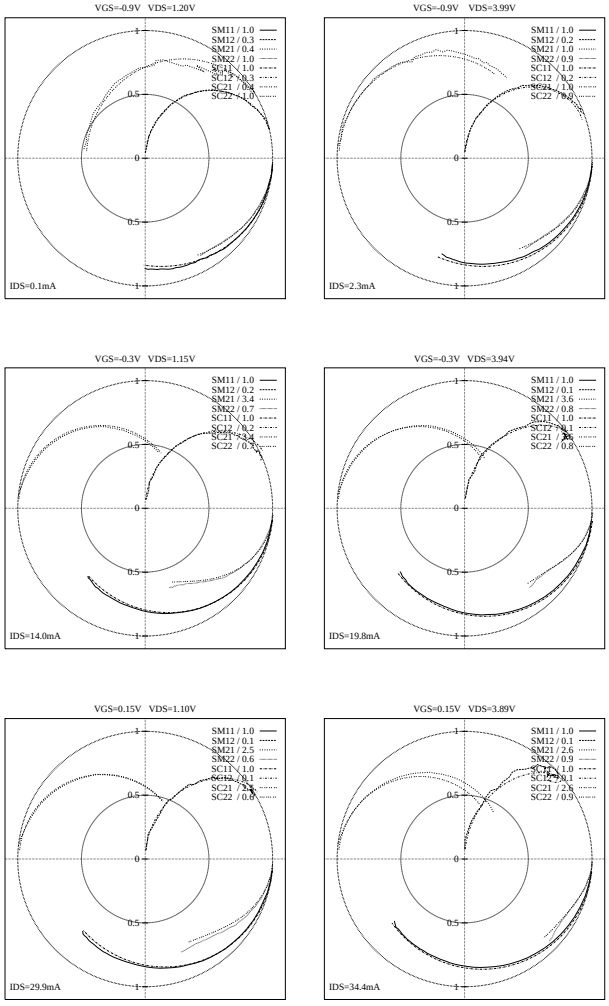

Fig. 6 : Normalized measured and modelled S–parameters for different bias situations, f =1–40 GHz, SM: measured, SC: computed.